



GROWTH OF ZnO NANOSTRUCTURES WITH DIFFERENT ALKALINE PRECURSOR SOLUTION

Ainun Rahmahwati Ainuddin and Wan Nur Amalina Mior Idris

Department of Material and Design Engineering, Faculty of Mechanical and Manufacturing Engineering, Universiti Tun Hussein Onn Malaysia, Parit Raja, Batu Pahat, Johor, Malaysia
E-Mail: ainun@uthm.edu.my

ABSTRACT

Nanostructures Zinc Oxide (ZnO) are promising candidates for novel application in solar cells, sensors, emerging transistors and optoelectronic devices. ZnO nanostructures have been successfully synthesized by using the hydrothermal technique on Zn substrates at 120 °C. The effect of synthesis condition from different deposition times and pH of alkaline precursor which played a role in the crystallization process were studied by scanning electron microscopy, X-ray diffraction spectra and atomic force microscopy. The I-V characteristic of the ZnO nanostructures were characterized with solar simulator. The results demonstrate that the morphology of ZnO nanostructures are determined by the growth temperature, the overall concentration of the precursors and deposition time. The formation mechanisms of different ZnO morphologies were also investigated based on the experimental results.

Keywords: zinc oxide, hydrothermal, pH, KOH, nanostructure.

INTRODUCTION

Zinc Oxide (ZnO) has a wide number of properties which has gained considerable attention from researchers over the past few years. ZnO is a popular material used in semiconductor research and this was mentioned back in 1945 (Gomez and Tigli, 2012). World-wide use of ZnO that has 9 % of metallic zinc is more than 1.2 million tonnes per year (International Zinc Association, 2011). Due to its unique chemical properties and structure, ZnO is increasingly being used in the production of electronic devices. The applications of ZnO are not only limited to the engineering field, but also the pharmaceutical industry, cosmetic and food packaging industry (Houng *et al.*, 2007; Rani *et al.*, 2008).

There are two types of synthesis methods to obtain the ZnO nanostructure. The ways are solution phase synthesis and gas phase synthesis. For solution phase synthesis, normally the aqueous solution is used and the process is referred to as hydrothermal growth process. Baruah and Dutta (2009) in their research said that solution phase synthesis processes consist of several methods; (i) Zinc Acetate Hydrate (ZAH) is derived from nano-colloidal sol-gel route, (ii) ZAH in alcoholic solutions with Sodium Hydroxide (NaOH), (iii) template assisted growth, (iv) spray pyrolysis for growth of thin films, and (v) electrophoresis. Due to the variety in methods, the structure and look of ZnO produced could be different. The best structure of ZnO is nanowire because of its good performance in electronics, optics and photons field (Zhang *et al.*, 2012). Hydrothermal synthesis is a robust and economic method for the growth ZnO nanowires that can be carried out with simple equipment unlike the other methods mentioned (Akgun *et al.*, 2012; Tong *et al.*, 2006; Liu *et al.*, 2005).

The properties of zinc oxide strongly depend on the synthesis method and conditions during processing. It is therefore critically important to develop synthetic strategies that control both size and shape while at the same time yielding materials with well-defined

compositions and structural morphologies. Moreover, the size and shape of the structures grown by this synthesis can be controlled by adjusting the growth parameters such as concentration of solution, reagents stoichiometry, temperature and pH (Sambath *et al.*, 2012; Pei *et al.*, 2010).

In this work, we focused on the fabrication of ZnO nanostructures via hydrothermal synthesis and the effects of alkaline solution on the morphologies. The ZnO nanostructures obtained after hydrothermal deposition of 6, 12 and 24h were produced in order to systematically investigate the effect of prolonged growth time on the structural and crystallinity by varying pH.

MATERIAL AND METHODS

Zinc foils (10 mm × 10 mm × 0.5 mm), used as both a solid reagent and as substrates for the direct growth of nanostructured ZnO films, were carefully cleaned in acetone containing ultrasound baths for 20 minutes. Prior to hydrothermal deposition the Zn foils were chemically etch using hydrochloric acid (HCl) in ethanol (EtOH) for 3 minutes. Purpose of etching process was to remove unwanted substances from the foils.

Concurrently, potassium hydroxide (KOH) (Kanto Chemical, 99%) solution was added with deionized (DI) water to form precursor solution until the pH values were 10 and 12. The precursor solutions were put in Teflon-lined stainless steel autoclaves and the clean Zn foils were added to each solution. The autoclaves were tightly closed, heated at 120 °C for 6, 12 and 24 h before left to cool down to room temperature. The as-synthesized films on Zn substrates were rinsed with DI water several times and dried at 60 °C for 3 h.

The crystallinity and phases of the ZnO nanostructures were characterized by an X-ray diffractometer (XRD, PANalytical X'Pert Powder) using Cu-K α radiation in the range of 20 to 80° while the surface morphologies were characterized by field emission scanning electron microscope (FE-SEM, JEOL JSM-



7600F) and atomic force microscope (AFM, Park Systems XE-100). The solar simulator (Newport type Sol 1A) was used to obtain the I-V characteristic of the ZnO nanostructured.

RESULTS AND DISCUSSIONS

Morphology and the structure of the hydrothermally derived ZnO nanostructures

The low magnification SEM images and their inserts as high magnification images of the ZnO nanostructures synthesized at the pH values of 10 and 12 at increasing deposition time were presented in Figure-1. Figure-1 also shows the different morphologies of the ZnO on Zn substrates. In this research, pencil-like, nano wire and nano rods ZnO were synthesized in KOH alkaline solution.

After 6 h of hydrothermal exposure in pH 10, pencil-like ZnO nanorods were observed from the surface morphology as shown in Figure-1(a). After 24 h of hydrothermal reaction, the average diameter of the nanorods decreased to form nanowires as shown in Figure-1(b). Increasing the pH value to 12, the ZnO nanostructures are observed as obelisk shaped ZnO nanorods as shown in Figure-1(c). Finally in Figure-1(d), further increase in hydrothermal reaction of pH value 12, a

blunt tip of multiple layered crystal structure of obelisk shaped ZnO nanorods occurred. Similar ZnO nanostructures also observed by other researcher in their synthesized (Li *et al.*, 2007; Wang *et al.*, 2004; Sambath *et al.*, 2012; Alias *et al.*, 2010).

From the above observations, it is obvious that the morphological characteristics of the ZnO nanostructures are distinctly controlled by the pH of the precursor and the deposition time. It was observed that the thickness and morphology of the ZnO nanorod arrays are affected by the alkalinity of the solution in the growth bath. The results can be related to AFM analysis.

Surface roughness of ZnO nanostructures were analyzed by AFM. Among the information that can be obtained from surface roughness analysis are average surface roughness (R_a) and root mean square roughness (R_q). Figure-2 shows the surface topologies of ZnO films with different pH values and deposition time by AFM measurements.

Scans of the few areas on the ZnO nanostructures surface shows the root mean square (RMS) roughness (R_q) were 286, 262 and 189 nm for pH value 10, while 98.32, 92.09 and 91.83 nm for pH value 12 with increasing deposition time from 6, 12 and 24 h, respectively. Based on the above RMS values, the surface roughness of KOH

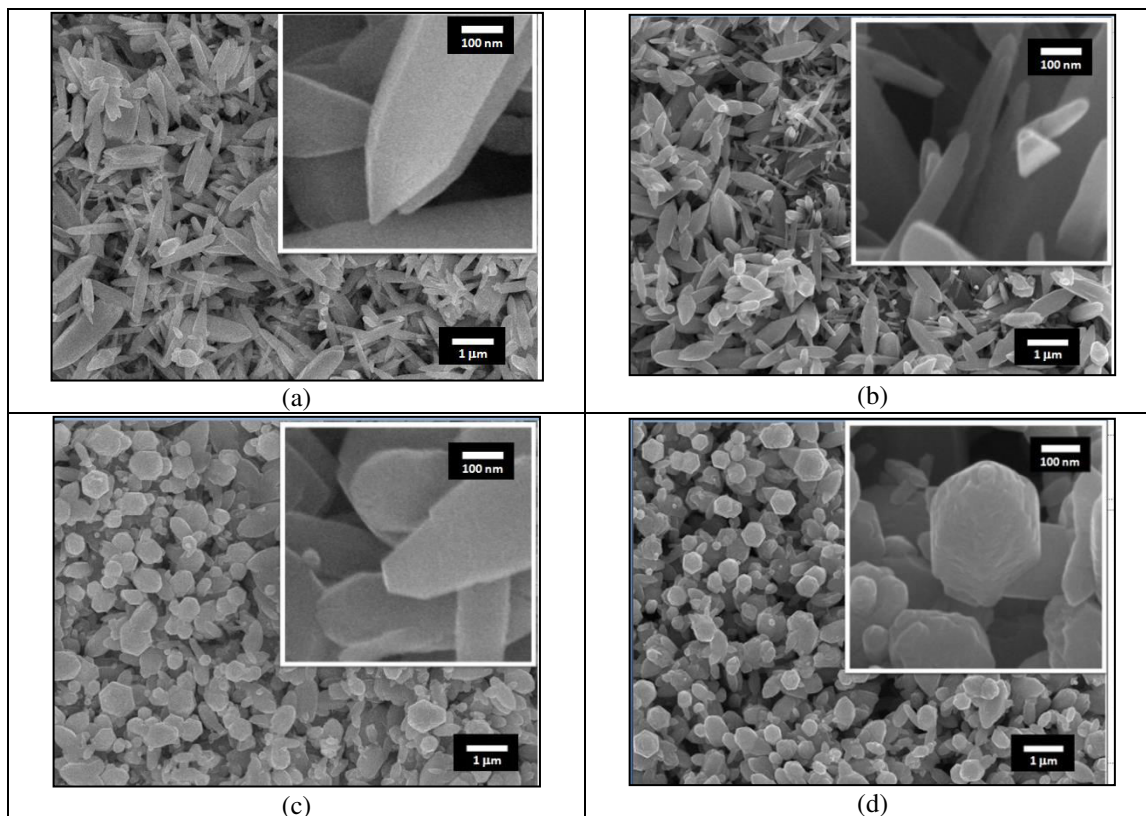


Figure-1. SEM images of ZnO nanostructures synthesized in KOH of (a) pH 10, 6 h; (b) pH 10, 24 h; (c) pH 12, 6 h and (d) pH 12 24 h deposition time.

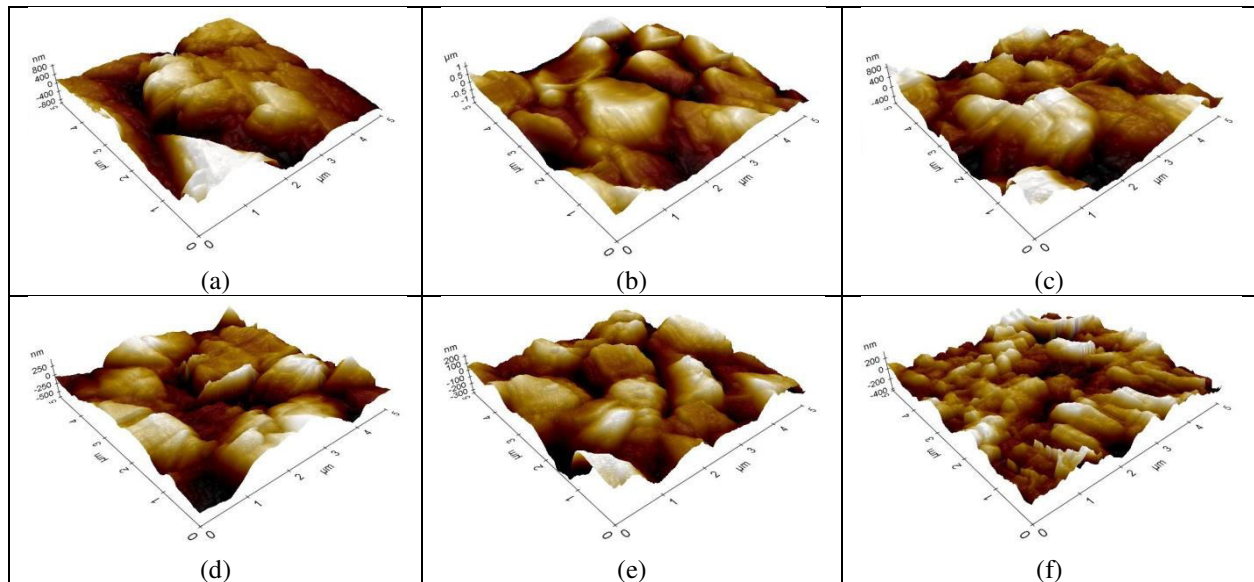


Figure-2. AFM images of ZnO nanostructures synthesized at (a) pH 10, 6 h; (b) pH 10, 12 h; (c) pH 10, 24 h; (d) pH 12, 6 h; (e) pH 12, 12 h and (f) pH 12, 24 h deposition time.

samples decreased due to the increase of pH value and hydrothermal process hours. There was a big difference in values of surface roughness for pH 10 and pH 12. The value of R_q for pH 12 was less than 100 nm compared to R_q values for pH 10. The surface morphology shows larger grains with the increase of pH value. This statement is supported by research conducted by Sagar *et al.* (2007).

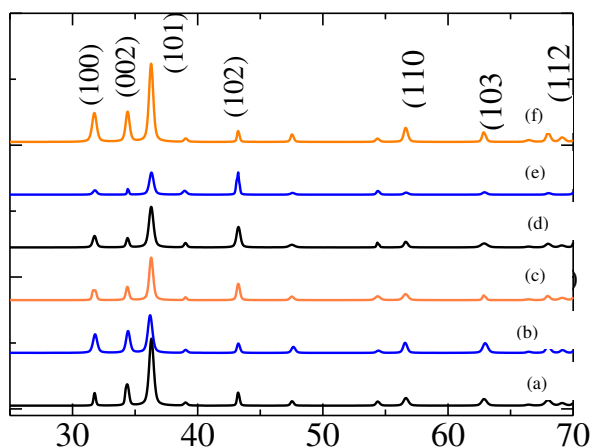


Figure-3. X-ray diffraction pattern of ZnO nanostructures prepared at (a) pH 10, 6 h; (b) pH 10, 12 h; (c) pH 10, 24 h; (d) pH 12, 6 h; (e) pH 12, 12 h and (f) pH 12, 24 h deposition time.

XRD observation

Figure-3 shows the X-ray diffraction pattern of ZnO as a function of increasing deposition time from 6, 12 and 24 h for pH value of 10 and 12. The detected (h k l) peaks were at 2θ values of 31.7, 34.4, 36.2, 47.5, 56.6, 62.8, and 67.6° corresponding to the lattice planes (100), (002), (101), (102), (110), (103) and (112), respectively. They are in agreement with the standard

JCPDS 036-1451 card for hexagonal wurtzite ZnO with the lattice parameter values of $a = 0.3250$ nm and $c = 0.5207$ nm.

The variation intensity of the diffraction peaks with the increasing pH and deposition time may be due to the formation of different ZnO nanostructured morphologies as shown by the SEM images. The absence of other peaks clearly suggests the formation of single phase ZnO. The strongest peak corresponds to the 101 plane is more prevalent for the nanostructures as reported by Sambath *et al.* (2012).

To calculate the grain sizes of ZnO nanostructures, D values which are related to the crystallite size were calculated according to the Scherrer from equation (1):

$$D = \frac{K\lambda}{B \cos \theta} \quad (1)$$

Where K = shape factor constant (0.9), λ = wavelength of the x-ray (1.5405600), $\cos \theta$ = cosine of half the 2θ angle, and B = broadening of diffraction line measured at half its maximum intensity (radians).

The grain size of ZnO nanostructures are found to be 41.6, 42.5, 48.5, 41.6, 44.8 and 45.8 nm for pH value 10 and 12 with deposition time of 6, 12 and 24 h, respectively. The average size is calculated using Scherrer formula. The improvement in grain size is in conformity with AFM results, where the morphology shows larger grains with the increase of pH (Sagar *et al.*, 2007).

Current against voltage measurement

The nanostructure of ZnO was analyzed using a 2-point probe equipment to measure the current against voltage. From the results of the voltage and current, the resistivity can be ascertained. Resistivity can be calculated from the value of voltage and current. Table-1 shows the



value of voltage, current and resistivity for all ZnO samples that underwent the hydrothermal process.

Based on the previous study from Shariffudin *et al.*, (2012), resistivity is closely related with the film thickness which is the thickness of ZnO layer that grow on the surface. The resistivity will increase with increasing film thickness. Besides that, the increased resistivity on ZnO thin film is caused by the porosity of the thin film. Hong *et al.*, (2013) found that increasing porosity decreases the electrical conductivity of ZnO. The higher the porosity occurring on ZnO nanostructures, the higher the resistivity.

Table-1. Results for the electrical properties of ZnO nanostructured.

Sample	Voc (V)	Isc (A)	Resistivity, $\rho(\Omega\text{m})$
a (pH10, 6 h)	0.02233	0.00136	0.16419
b (pH 10,12 h)	0.00832	0.00011	0.75636
c (pH10, 24 h)	0.00263	0.00004	0.65750
d (pH12, 6 h)	0.00482	0.00002	2.4100
e (pH 12, 12 h)	0.00585	0.00004	1.4625
f (pH12, 24 h)	0.00841	0.00006	1.40167

Based on the SEM images in Figure-1, the porosity on the ZnO nanostructures can be seen clearly. This clearly shows that the porosity in samples influenced the resistivity of this sample.

CONCLUSIONS

Based on the study done on pure Zn foil, it is proven that parameters such as the duration for hydrothermal process, types and the pH concentration of alkaline solutions are able to influence the characteristics of ZnO nanostructures. The use of alkaline solutions greatly affected the growth of ZnO nanostructures. The longer time of application for hydrothermal processes is required to produce a good formation of nanostructure when using weak alkaline solution as a precursor. Higher values of pH solutions were used to help the ZnO layer growth on Zn foils. Using hydrothermal synthesis, the production of ZnO becomes more environmentally friendly.

ACKNOWLEDGEMENTS

The authors would like to thanks Ministry of Higher Education of Malaysia for providing research funding support (ERGS Grant Vot No. E027) and Universiti Tun Hussein Onn Malaysia.

REFERENCES

- [1] Akgun M. C., Kalay Y. E., and Unalan H. E. 2012. Hydrothermal zinc oxide nanowire growth using zinc acetate dihydrate salt. *J Mater Res.* 27 (11), pp. 1445-1451.
- [2] Alias, S.S., Ismail, A. B., and Mohamad, A. A. 2010. Effect of pH on ZnO nanoparticle properties synthesized by sol-gel centrifugation. *J Alloys Compd.* (499), pp. 231-237.
- [3] Baruah, S., and Dutta, J. 2009. Hydrothermal growth of ZnO nanostructures. *Sci Technol Adv Mater*, 10(1), pp. 013001.
- [4] Gomez, J. L. and Tigli, O. 2012. Zinc oxide nanostructures: from growth to application. *J Mater Sci.*, 48(2), pp. 612-624.
- [5] Hong, Y., Tian, C., Jiang, B., Wu, A., Zhang, Q., Tian, G. and Fu, H., 2013. Facile synthesis of sheet-like ZnO assembly composed of small ZnO particles for highly efficient photocatalysis. *J Mater Chem A.* (1) pp. 5700-5708.
- [6] Houn, B., Huang, C. L., and Tsai, S. Y. 2007. Effect of the pH on the growth and properties of sol-gel derived boron-doped ZnO transparent conducting thin film. *J Cryst Growth*, 307(2), pp. 328-333.
- [7] International Zinc Association. 2011. Retrieved 30 October, 2014, from Zinc Website: http://www.zinc.org/info/zinc_oxide_applications.
- [8] Li, Z., Huang, X., Liu, J., Li, Y., Ji, X., and Li, G. 2007. Growth and comparison of different morphologic ZnO nanorod arrays by a simple aqueous solution route. *Mater. Lett.* (61) pp. 4362.
- [9] Liu, X., Jin, Z., Bu, S., Zhao, J., and Liu, Z. 2005. Effect of Buffer Layer on Solution deposited ZnO Films. *Mater Lett.* (59), 3994-3999.
- [10] Musić, S., Dragčević, D., Popović, S., and Ivanda, M. 2005. Precipitation of ZnO particles and their properties. *Mater. Lett.* (59), pp. 2388-2393.
- [11] Pei, L. Z., Zhao, H. S., Tan, W., Yu, H. Y., Chen, Y. W., Fan, C. G., and Zhang, Q. F. 2010. Hydrothermal oxidization preparation of ZnO nanorods on zinc substrate. *Physica E.* 42(5), pp. 1333-1337.
- [12] Rani, S., Suri, P., Shishodia, P. K., and Mehra, R. M. 2008. Synthesis of nanocrystalline ZnO powder via sol-gel route for dye-sensitized solar cells. *Sol Energy Mater Sol Cells*, 92(12), pp. 1639.-1645.
- [13] Sagar, P., Shishodia, P. K., and Mehra, R. M. 2007. Influence of pH value on the quality of sol-gel derived ZnO films. *Appl Surf Sci.* (253), pp. 5419-5424.



- [14] Sambath, K., Saroja, M., Venkatachalam, M., Rajendran, K. and Muthukumarasamy, N. 2012. Morphology controlled synthesis of ZnO nanostructures by varying pH. *J Mater Sci Mater Electron* (23), pp. 431-436.
- [15] Shariffudin, S. S., Salina, M., Herman, S. H., and Rusop, M. 2012. Effect of Film Thickness on Structural, Electrical, and Optical Properties of Sol-Gel Deposited Layer-by-layer ZnO Nanoparticles. *Trans Electr Electron Mater.* 13(2), pp. 102-105.
- [16] Tong, Y., Liu, Y., Dong, L., Zhao, D., Zhang, J., Lu, Y., Shen, D., and Fan, X. 2006. Growth of ZnO Nanostructures with Different Morphologies by Using Hydrothermal Technique. *J. Phys. Chem. B.* (110), pp. 20263-20267.
- [17] Wang, Z., Qian, X. F., Yin, J., and Zhu, Z. K. 2004. Large-Scale Fabrication of Tower-like, Flower-like, and Tube-like ZnO Arrays by a Simple Chemical Solution Route. *Langmuir* (20) pp. 3441-3448.
- [18] Zhang, Y., Ram, M.K., Elias, K., and Goswami, D.Y. 2012. Synthesis, Characterization, and Applications of ZnO Nanowires. *JNanomater.* 2012 p. 22.